Dynamic Viscoelastic Behavior of Polypropylene/ Polybutene-1 Blends and Its Correlation with Morphology

Farzaneh Ardakani, Yousef Jahani, Jalil Morshedian

Faculty of Processing, Iran Polymer and Petrochemical Institute, Tehran, Iran

Received 9 August 2011; accepted 26 September 2011
DOI 10.1002/app.36324
Published online 26 December 2011 in Wiley Online Library (wileyonlinelibrary.com).

ABSTRACT: In this study the rheology, morphology, and interfacial interaction of polypropylene (PP)/polybutene-1 (PB-1) blends in different percentages of PB-1 are investigated. The morphology of cryo-fractured surfaces of samples was studied by scanning electron microscopy (SEM). The SEM images showed a droplet-matrix structure in all range of compositions and the size of dispersed phase increased proportionally with PB-1 content. The miscibility of blends at various compositions is evaluated by viscoelastic parameters determined by dynamic oscillation rheometry in the linear viscoelastic region. A distinct Newtonian plateau at low frequencies is observed and the variations of complex viscosity (η^*) against angular frequency (ω) for all blends are in agreement with Cross model. The complex viscosity of samples at various percentages of PB-1 showed the log-additivity mixing rule behavior in low frequencies and positive-negative deviation behavior (PNDB) at high shear rates. The phenomena such as decrease in the sensitivity of storage modulus to shear rate in the terminal region, the deviation of Cole–Cole plots from the semi-circular shape, and the tail in relaxation spectrums at high relaxation times are the evidences of two phase heterogenous morphology. The effect of time–temperature on the phase behavior is studied and the interfacial tension between matrix and dispersed phase was evaluated by using emulsion theoretical models. J Appl Polym Sci 125: 640–648, 2012

Key words: polypropylene; polybutene-1; miscibility; morphology; rheology; interfacial tension

INTRODUCTION

Polypropylene is a commercially attractive plastic due to its good mechanical properties, excellent chemical resistance, and good processability with reasonable price.[1] Polybutene-1 can improve the impact strength, tear strength, puncture resistance, optical properties,[2,3] flow characteristics, creep, and ultimate elongation of PP with excellent heat sealability,[4,5] and enhanced weld line strength.

The miscibility of polyolefin blends in molten state affects the final performance and it sounds attractive to industries. It is generally accepted that, miscibility in polymer blends must be supported by the existence of specific interactions between the components. The miscibility and compatibility of PP and PB-1 blends was the subject of various studies.[6,7–9] It has been reported that there are not any specific interactions between PP and PB-1 in the blends, and the balance between dispersive and entropic driving force implies miscibility in some compositions.[10] The miscibility and compatibility of the PP/PB-1 blends has been evaluated by measuring the glass transition temperature, T_g, by dynamic mechanical analysis (DMA).[8] As they have been observed a single glass transition temperature over the entire composition ranges, it is concluded that these two polymers are miscible.[8] It is necessary to note that the T_g of PP and PB-1 is close to each other and their difference is less than 20°C, about 13–16.5°C,[11] and due to the broadness of PB-1 damping peak, DMA method is not capable to differentiate the damping peaks for T_g of blend's pair and consequently it is not accurate enough to announce the miscibility and compatibility of these two polymers. In another study, according to the results obtained by differential scanning calorimetry (DSC), thermo mechanical analysis (TMA), and based on the statistical calculations, it has been concluded that the PP and PB-1 are compatible.[9] The depression of the melting temperature and crystallization rate of PP are used to study the compatibility of this blend. It is concluded that PB-1 as a miscible diluents affect the crystallization behavior of PP and the two components are compatible in the amorphous phase.[7–12]

There are also some contradictory reports on the miscibility of PP/PB-1 blends.[13] In a study, it is detected two glass transition temperature (T_g) in ultra quenched samples prepared by compression molding process. According to these observations they have concluded that, PP and PB-1 are highly compatible but the miscibility by ordinary melt mixing process is difficult to obtain. The percentage of

Correspondence to: Y. Jahani (y.jahani@ippi.ac.ir).

PB-1 may also affect the miscibility and compatibility of the components.[14] It has been shown that the blends can be miscible in PB-1 content less that 20 wt % or higher than 80 wt % and immiscible in the middle composition range. Referring to this fact that the DSC and DMA techniques are incapable to detect the micro-heterogeneities smaller than 50 nm in the blends, a single T_g in a blend cannot be attributed to the miscibility in molecular level and should be confirmed by other analytical methods.[15]

It is known that rheology is an effective method to characterize the phase behavior of multicomponent polymer systems,[16,17] nevertheless, there is not available any released report on the rheological study of PP/PB-1 blends.

In this work, the dynamic viscoelastic parameters are determined by rheological test and the interfacial interaction of PP and PB-1 is evaluated by the emulsion theoretical models and correlated to the morphology. The miscibility, phase behavior, and flow properties of the blends are investigated at various temperatures and compositions.

EXPERIMENTAL

Materials

The PP used in this work was a homopolymer (Moplen HP500H) of Arak Petrochemical Company, Iran, with melt flow index of 2 g/10 min (230°C; 2.16 kg) and a homo Polybutene-1 (PB 0300M) with melt flow index of 4 g/10 min (190°C; 2.16 kg) and density of 0.915 g cm^{-3} is supplied by Lyondell Basell, Germany, as pellets.

Sample preparation

All blends were prepared in a predetermined weight percentages in different compositions of PB-1 (5, 10, 15, 20, 40, 60 wt %). The physically hand mixed granules were blended in a $L/D = 40$, corotating twin-screw lab extruder of Brabender, Germany. The mixing is carried out at 60 rpm and the temperature profile of 180–200°C from the hopper to die. The same compounding conditions are applied for both of neat PP and PB-1 resins, and also the blends, to ensure a unique thermo-mechanical history.

Morphological analysis

The morphology of the PP/PB-1 blend was studied by scanning electron microscope (SEM, VEGA\\ TESCAN, Czech Republic). The cryo-fractured samples in liquid nitrogen were kept immersed in cyclohexane for 30 min at 50°C, to remove the PB-1 from the fractured surface.[8] Samples were washed with fresh cyclohexane, dried, and gold coated prior to SEM test. The number and weight average diameter of 600 particles of dispersed phase was determined by using the SEM image analyzer.

Rheological studies

Rheological measurements were carried out on the neat polymers and the samples, using a Rheometrics Mechanical Spectrometer (RMS 800) on the 25-mm diameter disc obtained from the 1.5-mm injection-molded sheets in oscillation mode. Linear viscoelastic behavior of the samples was investigated in a frequency range of 0.01–600 rad s^{-1} with strain amplitude of 5%. The linear viscoelastic range of deformations was characterized by strain sweep test at the frequency of 10 rad s^{-1} at 180°C. All the samples were tested under nitrogen atmosphere to minimize oxidative degradation of the blends.

RESULTS AND DISCUSSION

Morphological properties

The SEM micrographs of the blends are shown in Figure 1(a–e). It is obvious that all samples have two-phase structure with droplet-matrix morphology. At low percentages of PB-1 (5–10 wt %) the fine droplets, homogeneously dispersed in the PP matrix, with a mean particle size diameters of about 25 and 40 nm for 5 and 10 wt %, respectively. By increasing the percentages of PB-1 from 20 up to 60 wt %, an uneven nonhomogenous distribution of particles is evident in the images and the size of the droplets increased from 55 to 200 and 450 nm in 15, 20, and 40 wt % PB-1, respectively.

Rheological properties

The complex viscosity of samples against angular frequency at various percentages of PB-1 is shown in Figure 2. It is seen that the complex viscosity curves of the blends are between the neat PP and PB-1 resins. At low frequencies, all the samples showed a Newtonian plateau which is more distinct at higher PB-1 percentages and followed by the power-law-like behavior at higher frequencies. Referring to the viscosity behavior of samples in Figure 2, it can be expected that the Cross equation properly correlate the complex viscosity to frequency of the samples[18,19]:

$$\eta^*(\omega) = \frac{\eta_0}{[1 + (\lambda\omega)^{1-n}]} \quad (1)$$

where η_0* is the zero shear viscosity, η*; complex viscosity, ω; frequency, λ; relaxation time. The

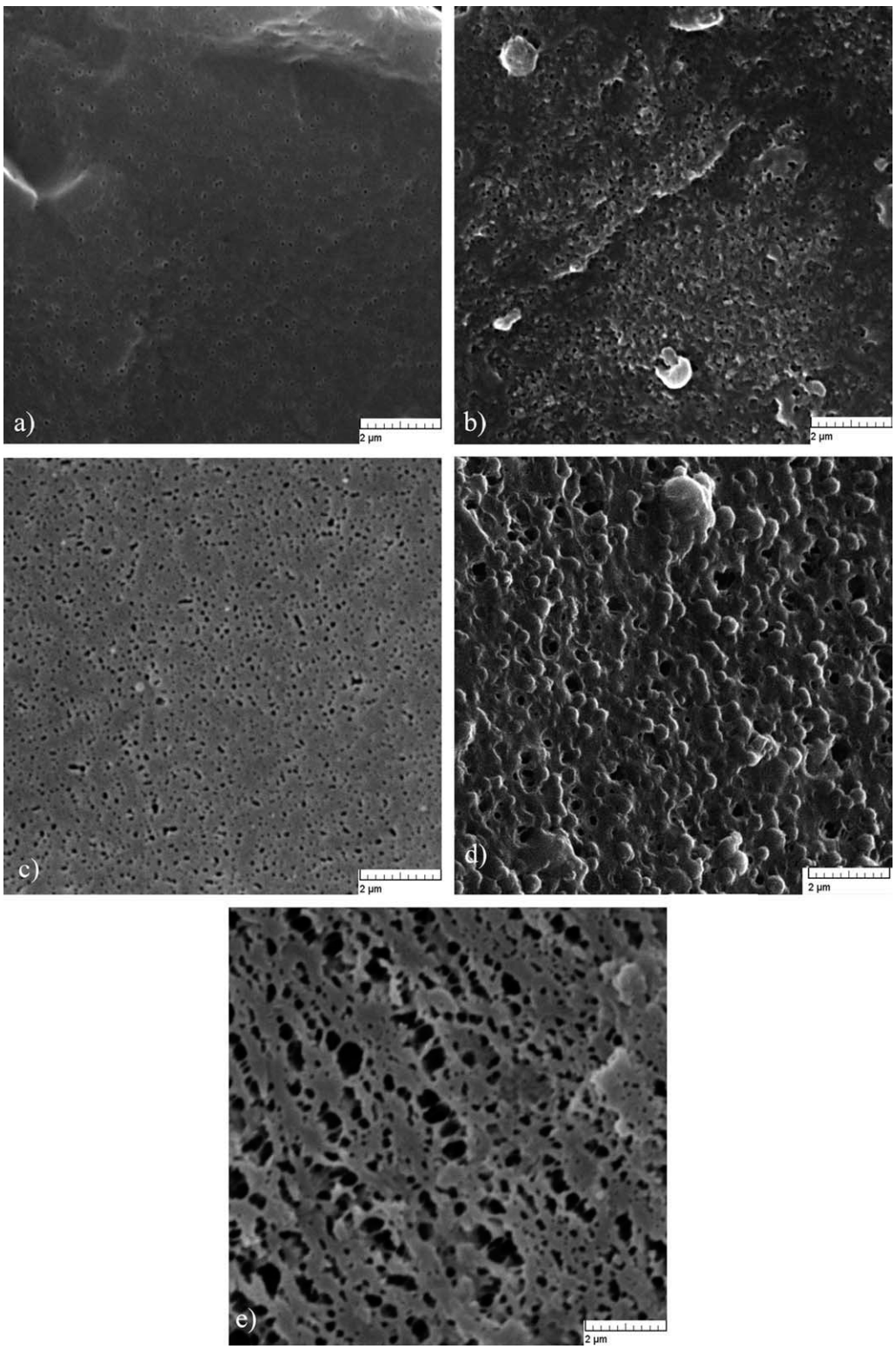

Figure 1 SEM microghraph of PP/PB-1 blends, (a) 5 wt %, (b) 10 wt %, (c) 15 wt %, (d) 20 wt %, (e) 40 wt % PB-1.

power-law index—*n*—can be determined by $\eta^* - \omega$ data at higher frequencies. The results of best fit of nonlinear regression of the eq. (1) are summarized in Table I. The theoretically predicted complex viscosity showed a good agreement with experimental data in all range of frequencies. The melt relaxation time of blends is decreased by increasing the PB-1 content from 1.7 s for neat PP resin, to 0.7 s for 60 wt % PB-1. The relaxation time obtained here by Cross equation are confirmed by weighted

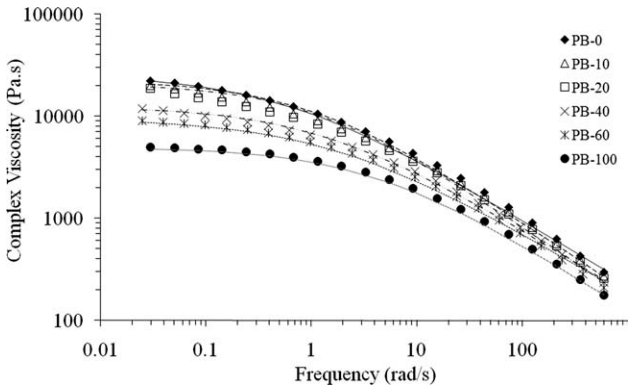

Figure 2 Complex viscosity versus frequency at 180°C (The lines related to the Cross model).

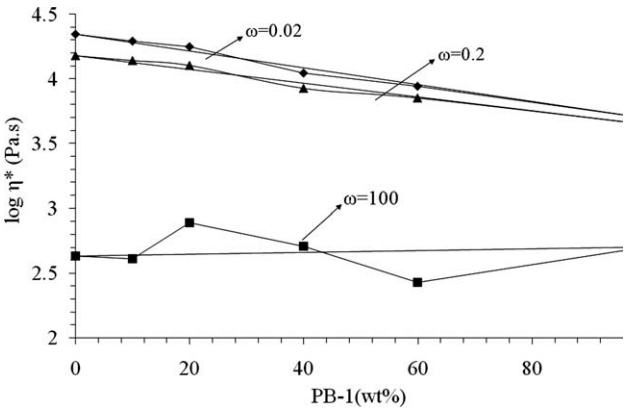

Figure 3 Logη* versus PB-1 composition in PP/PB-1 blend at 180°C in different shear rate.

relaxation time spectrum analysis represented in Figure 6.

The rheological data can be used to evaluate the miscibility and compatibility of polymer blends. The viscosity-composition behavior in polymer blends can be categorized in positive-deviation behavior (PDB), negative-deviation behavior (NDB) or positive-negative-deviation behavior (PNDB) by the log-additivity mixing rule.[20] It is suggested that showing PDB, is a sign of miscibility in polymer blends.[21] In spite of various attempts[21,22] it has found no exact relation between miscibility and viscosity-composition behavior in different polymer blends. For example, the PDB is found for the immiscible HDPE/LDPE and also HDPE/EVA blends, while for miscible poly-methylmethacrylate (PMMA)/poly-ethylene oxide (PEO) and poly(styrene-*co*-maleic anhydride) (SMA) the NDB was observed.[21] In Figure 3, the complex viscosity-compositions behavior of samples, at 180°C, is illustrated in three different frequencies of 0.02, 0.2, and 100 rad s^{-1}. At low frequencies (0.02, 0.2 rad s^{-1}) the complex viscosity-compositions showed a behavior nearly according to the log-additivity mixing rule and at high frequency (100 rad s^{-1}) it is deviated to the PNDB. The deviation from log-additivity mixing rule is significant at higher PB-1 concentration than 20 wt %, which is due to the larger droplets size of dispersed phase at higher concentrations. It has been proposed that,[22] the crossing point characteristic of PNDB curve and the line of log-additivity mixing rule is the composition of phase inversion phenomenon. This idea could not be investigated here in this work because there is no adequate solvent for PP that does not dissolve PB-1, therefore to prepare samples for SEM study the PP solely cannot be removed from the blends rich of PB-1.

TABLE I
Model Parameters of the Samples at 180°C

PB-1 (wt %)	n	λ	η_0 (Pa s^{-1})
0	0.37	1.7	24,200
10	0.33	1.1	23,000
20	0.32	0.9	21,000
40	0.36	0.7	12,500
60	0.39	0.6	9400
100	0.34	0.2	5000

The storage and loss modulus of neat resins and their blends at 180°C are shown in Figure 4(a,b). In the terminal region, the storage modulus of the blends containing 20–60 wt % of PB-1 is less

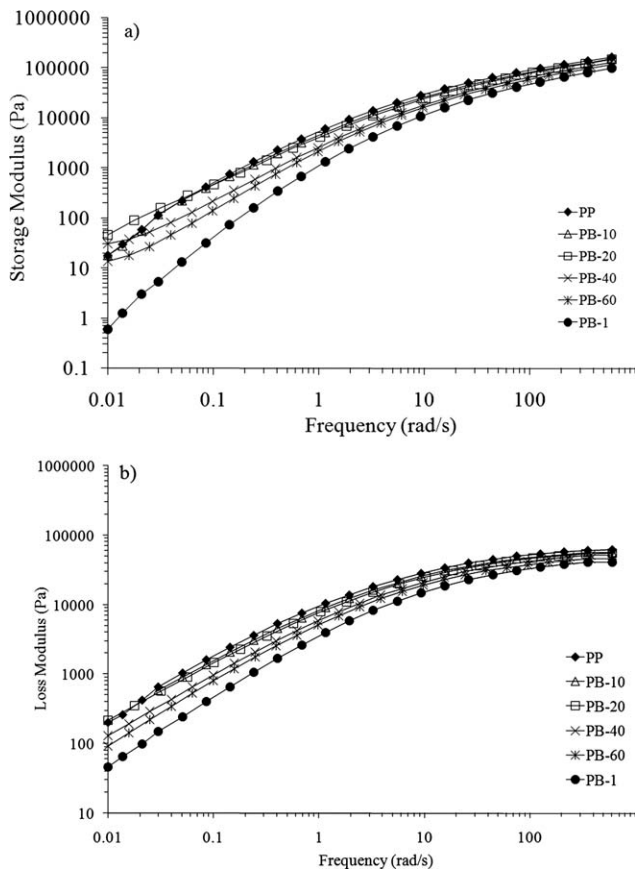

Figure 4 Dynamic modulus versus frequency for PP/PB-1 blends at 180°C.

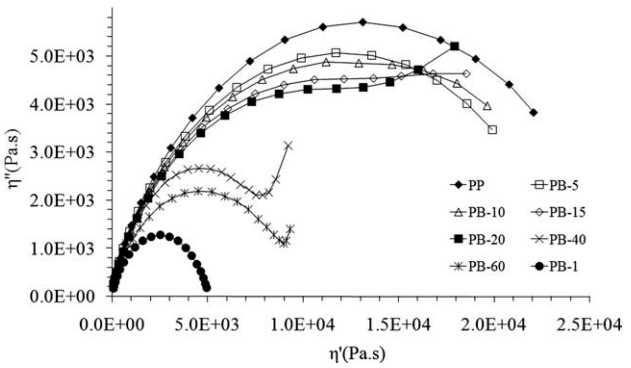

Figure 5 Cole–Cole plots for PP/PB-1 blends at 180°C.

sensitive to frequency changes than neat resins. The slope of $G' - \omega$ graphs in the terminal region are decreased which is pronounced at higher PB-1 content than 20 wt %. The increase of storage modulus and appearance of a secondary plateau at low frequencies in the terminal region as a fingerprint can be attributed to the heterogeneity in the polymer blends.[23–27] Graebling et al.[28] also observed that the secondary plateau at low frequency is related to size and amount of dispersed phase and width of this plateau is related to particle size distribution. This is due to oscillatory shear deformation of the PB-1 particles in the PP matrix and increased stored elastic energy.[29]

The Cole–Cole plot, η'' versus η', is a way to represent the miscibility and homogeneity of polymeric systems.[30–33] A single circular arc in the Cole–Cole curve denotes a homogeneous melt system; and if a shoulder or a second circular arc appears in the right-hand of the curve, it signifies the existence of a second phase and longer relaxation time.[26,33] Valenza et al.[28] observed that the particle size of dispersed phase and interfacial strength affects the shape of the Cole–Cole plot.

The Cole–Cole plots of samples are shown in Figure 5. As is seen, the Cole–Cole plots of samples up to 10 wt %, is nearly semicircular in shape. At higher PB-1 content than 10 wt % PB-1, the plots are deviated from semicircular shape by showing the increase of η'' against η', toward the neat PP resin, with a larger arc which is the evidence of two-phase morphology with two relaxation times.

The weighted relaxation spectrum, H(λ).λ, at 180°C were plotted against characteristic relaxation time, λ, in Figure 6. The relaxation spectrum, H(λ), was calculated from dynamic modulus data by Tschoegle approximation[27]:

$$H(\lambda) = G'\left[d\log G'/d\log\omega - \left(1/2\right)\left(d\log/d\log\omega\right) - \left(1/4.606\right)d^2\log G'/d\left(\log\omega\right)^2\right]_{\lambda=\sqrt{2}/\omega} \quad (2)$$

where ω is the frequency.

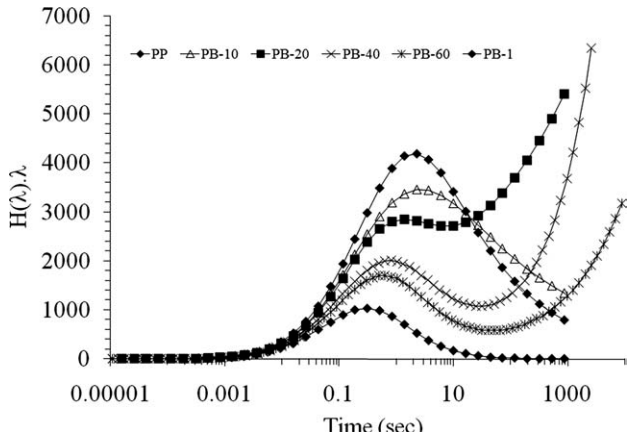

Figure 6 Weighted relaxation spectrum, $H(\lambda).\lambda$, of pure components and their blends at 180°C.

As is seen in Figure 6, the neat PP and PB-1 resins had different characteristic relaxation time due to their different rate of relaxation. The blends with 5–10 wt % PB-1 have the unique λ of about 0.5 s, with the PP matrix. At higher PB-1 concentration than 10 wt %, the λ of blends is shifted toward the λ of neat PB-1 resin (about 0.2 s). At higher PB-1 content than 10 wt % a distinct tail on the right-hand side of the weighted relaxation spectrum were observed representing another relaxation mechanism. This terminal behavior can be attributed to the presence of larger phase domains with different characteristic length scales and different relaxation times.[34,35]

This is in agreement with the observations in Cole–Cole plots of samples in Figure 5. It is known that the relaxation time spectrum of a blend is the result of relaxation time of matrix and dispersed phase. The longest relaxation time can be due to geometrical relaxation mechanisms of the dispersed phase's droplets,[36] and it can be referred to the formation of heterogeneous structure.[32] The characteristic relaxation time of the blends at various amount of PB-1 resin is shown in Figure 7. The longest

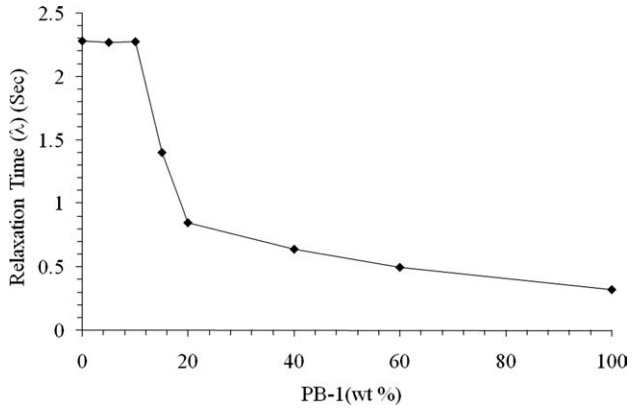

Figure 7 Relaxation time, λ, of blends in different composition of PB-1.

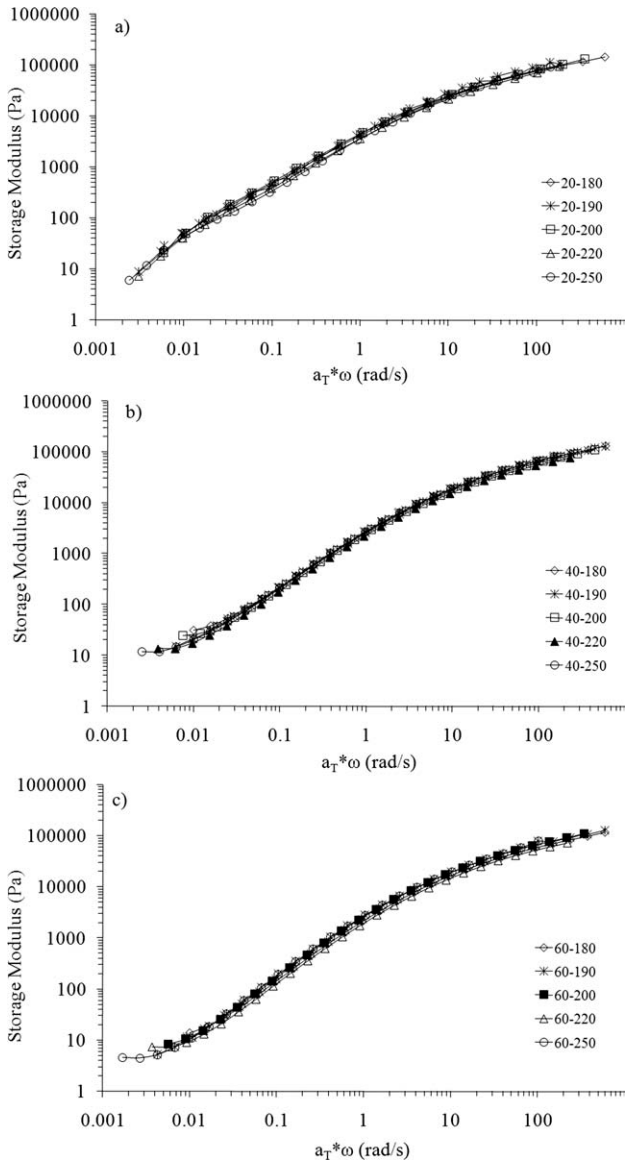

Figure 8 Master curve of storage modulus for PP/(a) 20, (b) 40, (c) 60 wt % PB-1 blend.

relaxation times can be several orders of magnitude longer than terminal relaxation times of the individual phases and were not detected here during the time span of our experiments.

Study of the homogeneity of blends by time temperature superposition

Time temperature superposition (TTS) is a well known method to determine the temperature dependency of the rheological behavior of a homopolymer or to expand the time or frequency regime at a given temperature at which the material behavior is studied.[37] However the TTS has been most commonly first used for homopolymers, later on it is applied to compatible blends with a single T_g. It may be necessary to note that it is valid when the morphology does not change over the temperature range of experiments therefore it can be used to study the homogeneity of polymer blends. It is believed that the heterogeneous polymeric systems, because of the different temperature dependencies of the components, do not imitate the TTS rule.[38] Nevertheless some contradictory results have been found. It has been reported that the behavior of miscible blends, such as polyethylene oxide (PEO)/polymethyl methacrylate (PMMA)[39] and 1,2-polybutadiene (PB)/1,4-polyisoprene (PIP),[40] is not according to TTS rule,[37,38] and consequently it can not be proposed a general relationship between TTS rule and the miscibility in polymer blends.

Figure 8(a–c) shows that the PP/PB-1 blends in all composition obey the TTS rule. To construct the master curve, the horizontal shift factors, (a_T) were determined by measuring the shift of $G^* - \omega$ curves at 180°C up to 250°C against reference temperature of 190°C. The G''–G' plot for the blends was temperature independent; therefore the vertical shift was not necessary.[39] An Arrhenius type behavior is found for the horizontal shift factor according to eq. (3):

$$a_T = \exp\left(\frac{E_H}{R}\left(\frac{1}{T} - \frac{1}{T_{\text{ref}}}\right)\right) \tag{3}$$

where a_T is horizontal shift factor; E_H, horizontal flow activation energy; R, universal gas constant; T, temperature; and T_{ref}, reference temperature.

The horizontal shift factors and flow activation energies of each component and their blends are shown in Table II. To increase the accuracy of the TTS validity test, the analysis of Van Gurp-Palmen[38] was used. As depicted by Van Gurp-Palmen plot in Figure 9(a–c) all of the data define a single line that is the evidence of adherence of TTS rule. This is typical simple thermorheological behaviors that confirm the validity of the TTS rule.[39]

Macaubas reported that the applicability of TTS in polymer blends can be related to the proximity of the E_H and a_T of the components in the systems.[41] As Showed in Table II, these parameters determined

TABLE II
Time–Temperature Superposition Parameters

Polymer	PP	PB-1	PB-20	PB-40	PB-60
TTS holds	Yes	Yes	Yes	Yes	Yes
a_T 180°C	1	1	1	1	1
a_T 190°C	0.765	0.743	0.795	0.905	0.746
a_T 200°C	0.596	0.543	0.593	0.751	0.572
a_T 220°C	0.397	0.271	0.305	0.391	0.371
a_T 250°C	0.243	0.095	0.237	0.252	0.169
E_H (Kj mol^{-1})	19.2	22.9	42.9	41.7	49.3

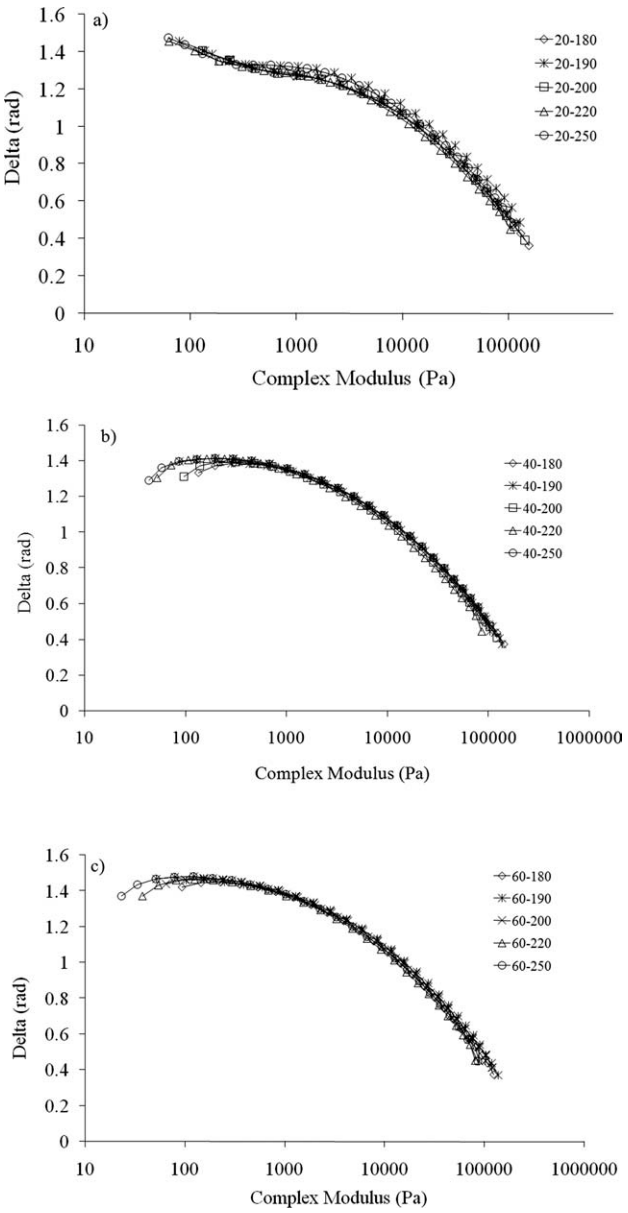

Figure 9 Van Gurp-Palman plot for PP/(a) 20, (b) 40, (c) 60 wt % PB-1 blend.

for PP and PB-1 are close to each other and can be attributed to the validity of TTS rule for this blend.

It is found that the PP/PB-1 blends have heterogeneous two phase structure with droplet-matrix morphology but due to similarity in temperature dependencies of PP and PB-1, which can be due to similarity of their E_H and a_T, they can be classified in the category of blends that in spite of their immiscibility obey TTS rule.

Quantitative evaluation of interfacial interaction

There are many theoretical models that have been developed to predict the linear viscoelastic behavior of polymer blends.[41] These models relate the dynamic response of polymer blends to their morphology, composition, and interfacial tension between the components. Einstein[42] predicted the viscosity of the dilute suspension of small solid spheres in a Newtonian fluid.[43] Taylor[44] proposed an extended theory including the case of the dilute emulsion in which spheres are liquid. He assumed that the interfacial tension is sufficiently strong that the droplets can keep their spherical shape. Then Schowalter[45] have applied Taylor's work for the deformable suspended droplets in Newtonian fluids, and Brenner[46] has obtained the complete solution of this problem in the linear viscoelastic range of deformation. According to these results, the dynamic moduli of the dilute emulsions of Newtonian liquids for a small-amplitude dynamic shear experiment can be expressed as:

$$G'(\omega) = \frac{\eta_0^0 R\varphi}{80\sigma}\left(\frac{19K+16}{K+1}\right)^2\omega^2 \tag{4}$$

$$G''(\omega) = \eta_0^0\left(1+\left(\frac{5K+2}{2K+2}\right)\varphi\right)\omega \tag{5}$$

where η_0^0 is the zero shear viscosity of the matrix, K is the ratio of zero shear viscosity of inclusions to the matrix ($K = \eta_i^0/\eta_0^0$), R is the radius of inclusions assumed to be monodisperese in size, and σ is the interfacial tension. ϕ and ω are the volume fraction of inclusion and the frequency, respectively. Oldroyd[47,48] extended Taylor analysis and made a calculation of the macroscopic elastic properties of a dilute emulsion arising from the interfacial tension between the two Newtonian fluids. The assumptions in this equation are that the deformable particles are fine and have uniform size. The equation obtained from his calculation is:

$$G^* = G_M^*\left(\frac{1+3\varphi H}{1-2\varphi H}\right) \tag{6}$$

where

$$H = \frac{4\sigma/[R(2G_M^*+5G_d^*)] + (G_d^*-G_M^*)(16G_M^*+19G_d^*)}{40\sigma/[R(G_M^*+G_d^*)] + 2(G_d^*+3G_M^*)(16G_M^*+19G_d^*)} \tag{7}$$

where G^* is the complex modulus and ϕ, σ, and R designate the same parameters as given in eq. (4). The indices M and d denote the matrix and disperse phase, respectively. Palierne[49] derived the linear viscoelastic modulus at an arbitrary concentration for polydisperse spherical inclusions. In this model both the matrix and droplets are assumed to be viscoelastic. For dilute emulsion it is expressed as follows:

$$G^* = G_M^*\left(1+\frac{5}{2}\sum_i \varphi_i \frac{E_i}{D_i}\right) \quad (8)$$

where

$$E_i = 2(G_d^* - G_M^*)(19G_d^* + 16G_M^*) + 8\sigma/[R_i(5G_d^* + 2G_M^*)] \quad (9)$$

$$D_i = 2(G_d^* - 3G_M^*)(19G_d^* + 16G_M^*) + 40\sigma/[R_i(G_d^* + G_M^*)] \quad (10)$$

where ϕ_i is the volume fraction of Type i grouped by the size of polydisperse inclusions. This model is valid if the secondary plateau could be observed in the storage modulus curve.[27] The Palierne model reduces to the eq. (11) when the two emulsion viscoelastic phases have a uniform particle size and the interfacial tension is constant:

$$G_b^*(\omega) = G_M^*(\omega)\left(\frac{1+3\varphi H(\omega)}{1-2\varphi H(\omega)}\right)$$
$$H(\omega) = \frac{4(\sigma/R_v)[(2G_M^*(\omega)+5G_d^*(\omega))] + (G_d^*(\omega)-G_M^*(\omega))(16G_M^*(\omega)+19G_d^*(\omega))}{40(\sigma/R_v)[(G_M^*(\omega)+G_d^*(\omega))] + (2G_d^*(\omega)-3G_M^*(\omega))(16G_M^*(\omega)+19G_d^*(\omega))} \quad (11)$$

where G^*, ϕ, and σ designate the same parameters as given in eqs. (6) and (7). R_v is the volume fraction of droplets. b, M, and d denote the blend, matrix, and droplet, respectively.

Bousmina[50,51] extended Kerner's model[52] to viscoelastic media and derived a simple expression for the complex shear modulus of an emulsion consisting of two viscoelastic fluids:

$$G_b^* = G_M^*\frac{2[G_d^* + (\sigma/R)] + 3G_M^* + 3\varphi[G_d^* + (\sigma/R) - G_M^*]}{2[G_d^* + (\sigma/R)] + 3G_M^* - 2\varphi[G_d^* + (\sigma/R) - G_M^*]} \quad (12)$$

The Palierne and Bousmina model predictions are in good agreement with the experimental results of viscoelastic emulsions but fail as expected in the cases that strong particle–particle interactions or agglomerated particles are present.[53] The interfacial tension (σ) can be estimated by the experimentally determined dynamic modulus, radius of inclusions, and volume fraction. Because of the long equilibrium time of polymer blends and the risk of thermal degradation in their melt state, direct measurement of interfacial tension is complicated. Hence a few techniques such as pendant drop and the tensiometric method are known to be suitable for polymer systems.[54,55]

Using eq. (4), the σ values can be determined by applying zero shear viscosity and the average radius of inclusion determined from SEM micrographs at a specific blend ratio. However the values of σ determined by this method are not absolute, but its order of magnitude is meaningful. The σ values which show the best fit with the experimental data are obtained from eq. (4), and the predictions of eqs. (11) and (12) are compared with the experiment data. The models predictions for G' are compared with experimental data for PB-10 and PB-20 in Figure 10(a,b). No considerable differences were observed between the predictions of Palierne and Bousmina models. By using eq. (4), the interfacial tension between PP and PB-1 at 180°C was found to be 0.08 and 0.15 mN m^{-1}, respectively for blends containing 10 and 20 wt % PB-1.

At higher percentages of PB-1, such as PB-40 and PB-60 samples, the Palierne model fail to predict the storage modulus behavior while the Bousmina's

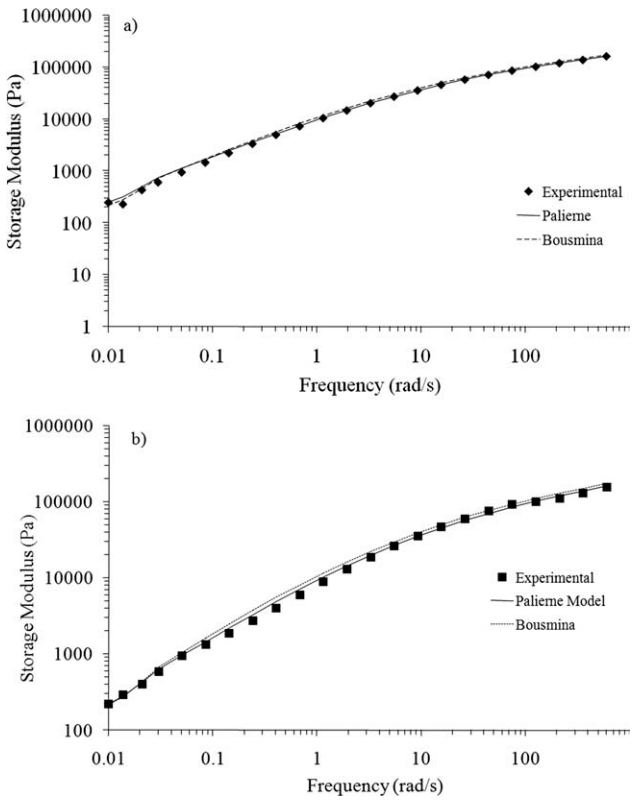

Figure 10 Comparison between experimental results and the emulsion model predictions for PP/ (a) 10 wt % PB-1, (b) 20 wt % PB-1 blends.

models prediction still are valid. It should be noted that the validity of Palierne model is limited to some assumptions. One of these assumptions is that the droplets of dispersed phase are nearly spherical. It is also hypothesized that the dispersed coefficient is lower than 2. The dispersed coefficient is R_v/R_n; $(\bar{R}_n = \frac{(\Sigma R_i)}{n_i})$, where n_i is the number of droplet with the radius of R_i. In PB-40 sample the droplets are non-homogeneous and the dispersed coefficient is higher than 2. So the Palierne emulsion model is supposed not to be in agreement with experimental data in this composition.

CONCLUSIONS

In this work the rheology and morphology of PP/PB-1 blends were investigated. This study leads to the following conclusions:

A droplet-matrix morphology was observed for all blends in SEM images. At low concentrations, up to 10 wt % PB-1, the particles size is smaller than 40 nm and homogenously dispersed in the matrix. By increasing the percentage of PB-1 a non-homogenous morphology is obtained and the size of the droplets increased.

At PB-1 contents higher than 10 wt % the sensitivity of storage modulus to shear rate was decreased, and a second plateau appeared in the terminal region that can be attributed to the heterogeneity in the blends. By increasing the size and amount of PB-1 phase the width of the plateau enhanced.

A single circular arc in the Cole–Cole plot of blends denotes a homogeneous melt system. The Cole–Cole plots of samples up to 10 wt %, was nearly semicircular and deviated from semicircular shape at higher PB-1 content than 10 wt %, It can be concluded that the Cole–Cole plot is not sensitive to nonhomogeneities with particle size smaller than about 40 nm.

The characteristic relaxation time of blends up to 10 wt % PB-1 is the same as λ of matrix/PP neat resin. It can be concluded that the fine droplets of dispersed phase in the range of 10 wt % PB-1 do not affect the characteristic relaxation time of blends.

The PP/PB-1 blends have heterogeneous two phase structure as is evident in SEM images. Because of similarity in molecular architecture and temperature dependencies of PP and PB-1 with nearly similar E_H and a_T, their blends obey TTS rule.

The interfacial tension determined by Palierne and Bousmina model was close to each other. By increasing the percentages of PB-1 in the blends the interfacial tension increased.

The authors wish to thank Lyondellbasell Company for its kind support and supplying the PB-1 resin.

References

1. Phillips, R. A.; Wolkowiez, M. D. Handbook of Polypropylene; Hanser: Munich, 2001; Chapter 3.
2. Schard, M. P.; Califon, N. J. U.S. Pat. 3,900,534, 1975.
3. White, J. L.; Choi, D. Polyolefines; Carl Hanser Verlag: Munich, 2001.
4. Turke, R. M.; Gryziecki, M. U.S. Pat. 5,041,491, 1991.
5. Kalay, G.; Kalay, C. R. J Appl Polym Sci 2003, 88, 806.
6. Siegmann, A. J Appl Polym Sci 1982, 27, 1053.
7. Piloz, A.; Decroix, J. Y. Angew Macromol Chem 1976, 54, 77.
8. Olabisi, O. Encyclopedia of Chemical Technology, 3rd ed.; Wiley: New York, 1982; Vol. 18, p 443.
9. Berticat, P.; Boiteux, G. Eur Polym J 1980, 16, 479.
10. Cham, P. M.; Lee, T. H.; Marand, H. Macromolecules 1994, 27, 4263.
11. Lee, M. S.; Chen, S. A. J Polym Res 1996, 3, 235.
12. Siegmann, A. J Appl Polym Sci 1979, 24, 2333.
13. Hsu, C. C.; Geil, P. H. Polym Eng Sci 1987, 27, 1542.
14. Gohil, R. M.; Petermann, J. J. Macromol Sci Phys 1980, B18, 217.
15. Han, C. D.; Kim, J. K. Polymer 1993, 34, 2533.
16. Zuo, M.; Zheng, Q. Macromol Chem Phys 2006, 207, 1927.
17. Polios, I.; Soliman, M. Macromolecules 1997, 30, 4470.
18. Dealy, J. M. Melt Rheology and its Role in Plastics Processing: Theory and Application; Kluwer Academic Publishers: Netherlands, 2006.
19. Cross, M. M. J Appl Polym Sci 1969, 13, 765.
20. Utraki, L. A.; Kamal, M. R. Polym Eng Sci 1982, 22, 96.
21. Kwak, H.; Rana, D. J Ind Eng Chem 2000, 6, 107.
22. Kammer, H. W.; Socher, M. Acta Polym 1982, 33, 658.
23. Li, R. M.; Yu, W.; Zhou, C. Polym Bull 2006, 56, 455.
24. Madbouly, S. A.; Qugizawa, T. J Macromol Sci Phys 2002, B41, 271.
25. Jeon, H. S.; Nakatani, A. I. Macromolecules 2000, 33, 9732.
26. Chopra, D.; Kontopoulou, M. Rheol Acta 2002, 41, 10.
27. Graebling, D.; Muller, R.; Palierne, J. F. J Phys IV 1993, 3, 1525.
28. Graebling, D.; Muller, R.; Palierne, J. F. Macromolecules 1993, 26, 320.
29. Colby, R. H. Polymer, 1989, 30, 1275.
30. Chopra, D.; Vlassopoulos, D. J Rheol 1998, 42, 1227.
31. Yu, F.; Zhang, H.; Zheng, H. Eur Polym J 2008, 44, 79.
32. Cho, K.; Lee, H.; Lee, B. H. Polym Eng Sci 1998, 38, 1969.
33. Zheng, Q.; Cao, Y. X. Chin J Polym Sci 2004, 22, 363.
34. Li, R.; Yu, W. J Macromol Sci B Phys 2006, 45, 889.
35. Delgadillo, O.; Sentmanat, M. Rheol Acta 2008, 47, 19.
36. Ajji, A.; Choplin, L.; Prudhomme, R. J Polym Sci B Polym Phys 1991, 29, 1573.
37. Colby, R. H. Polymer, 1989, 30, 1275.
38. Van Gurp, M.; Palmen, J. Rheol Bull 1998, 67, 5.
39. Roovers, J.; Toporowski, P. M. Macromolecules 1992, 25, 3454.
40. Souza, A. M. C.; Demarqutte, N. R. Polymer 2002, 43, 1313.
41. Macaubas, P. H. P.; Demarquette, N. R. Polym Eng Sci 2002, 42, 1509.
42. Hiemenz, P. C. Principle of Colloid and Surface Chemistry, 2nd ed.; Marcel Dekker: New York, 1986.
43. Kim, H. C.; Nam, K. H. Polymer 1993, 34, 4043.
44. Taylor, G. I. Proc R Soc Ser A 1932, 138, 41.
45. Schowalter, W. R.; Chaffey, C. E. J Colloid Interface Sci 1968, 26, 152.
46. Brenner, H. Chem Eng Sci 1964, 19, 519.
47. Oldroyd, J. G. Proc R Soc Ser A 1953, 218, 122.
48. Oldroyd, J. G. Proc R Soc Ser A 1955, 232, 567.
49. Palierne, J. F. Rheol Acta 1990, 29, 204.
50. Zuo, M.; Zheng, Q. Macromol Chem Phys 2006, 207, 1927.
51. Bousmina, M. Rheol Acta 1999, 38, 73.
52. Kerner, E. H. Proc Phys Soc 1956, A69, 808.
53. Lacroix, C.; Bousmina, M. Polymer 1996, 37, 2939.
54. Wu, S. Polymer Interface and Adhesion; Marcel Dekker: New York, 1982.
55. Lee, S. H.; Kontopoulou, M. Polymer 2010, 51, 1147.